

Adjoint-based Optimisation of a BWB Shape with Shock Control Bumps

Wai Sam Wong, Alan Le Moigne, Ning Qin

*Aerodynamics and Thermofluids Group
Department of Mechanical Engineering
The University of Sheffield, UK*

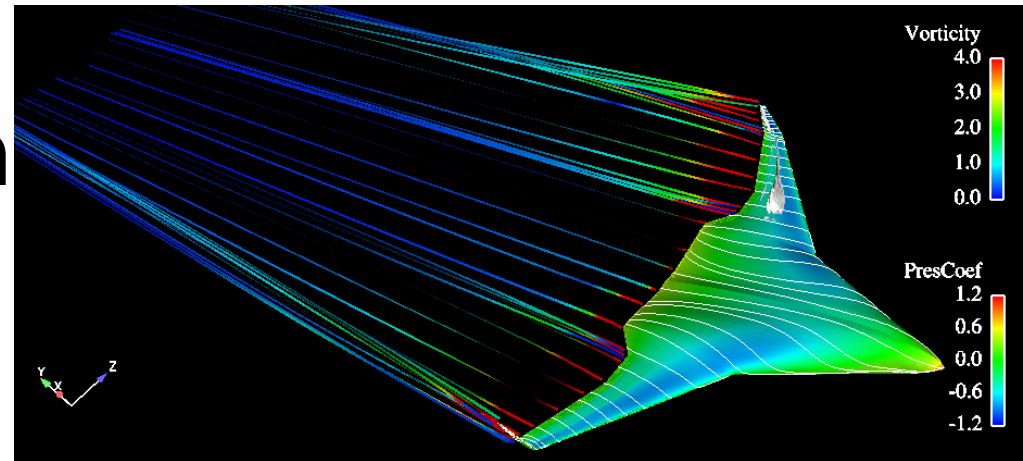
UKAA Consortium Conference, 5/6 April 2006



Presentation outline

- Background work
- Optimisation setup
- Parallelisation of flow solver, adjoint solver, grid deformation
- Optimisation results
- Concluding remarks

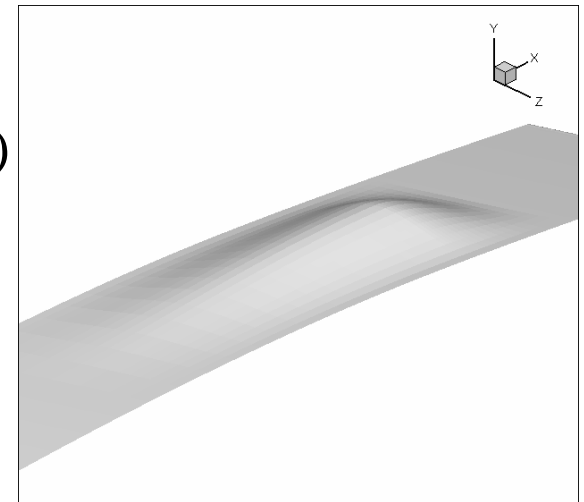
BWB Optimisation



- A candidate for future large transport aircraft ($M=0.85$)
- Shape optimisation can result in significant drag reduction for a given planform
- Aerodynamic shape optimisation has been used in multi-disciplinary optimisation within MOB project

Shock control bumps

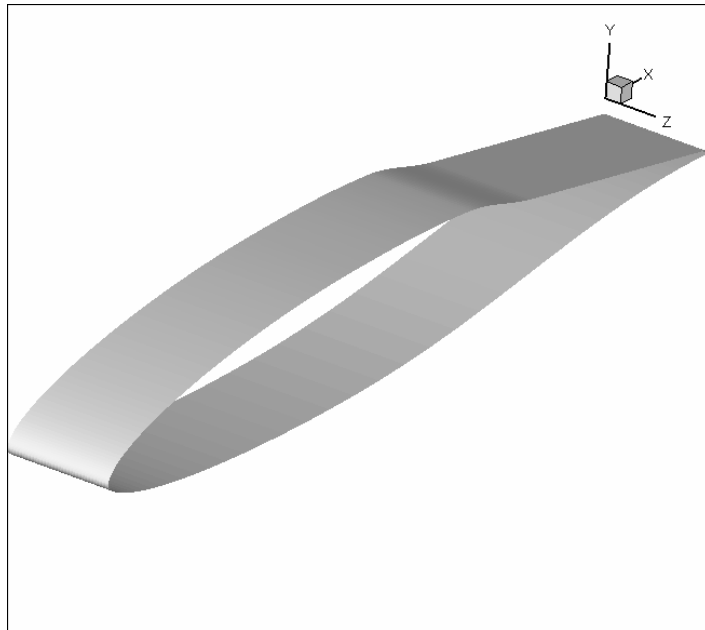
- During transonic flights, the presence of shock waves leads to an increase in drag.
- Drag rise Mach number and buffet boundary are determined by shock induced separation
- Shock control bumps were found effective in reducing wave drag and therefore total drag (~25%)
- 3D bumps were found to be beneficial over a wide range of operating conditions in comparison with 2D bumps.



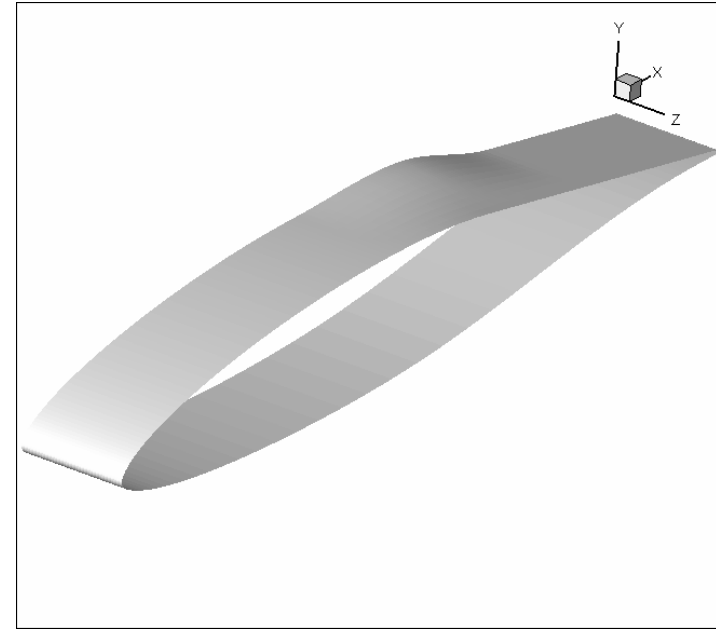
Shock Control Bumps on a 2D Wing

2D & 3D bumps are parameterised with four and six design variables, respectively.

NLF aerofoil (RAE 5243) wing with the bumps are shown here.



2D Bump



3D Bump

Lift Constrained Optimisations on RAE 5243 aerofoil

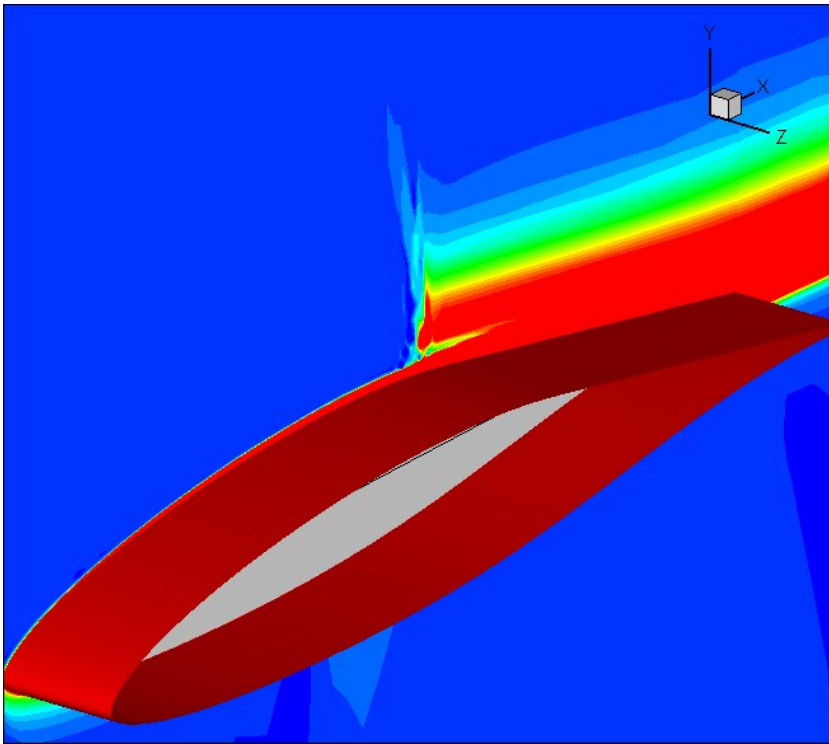
The design conditions are:

$$M = 0.68, Re_c = 19 \times 10^6, C_L = 0.82 (\text{constraint})$$

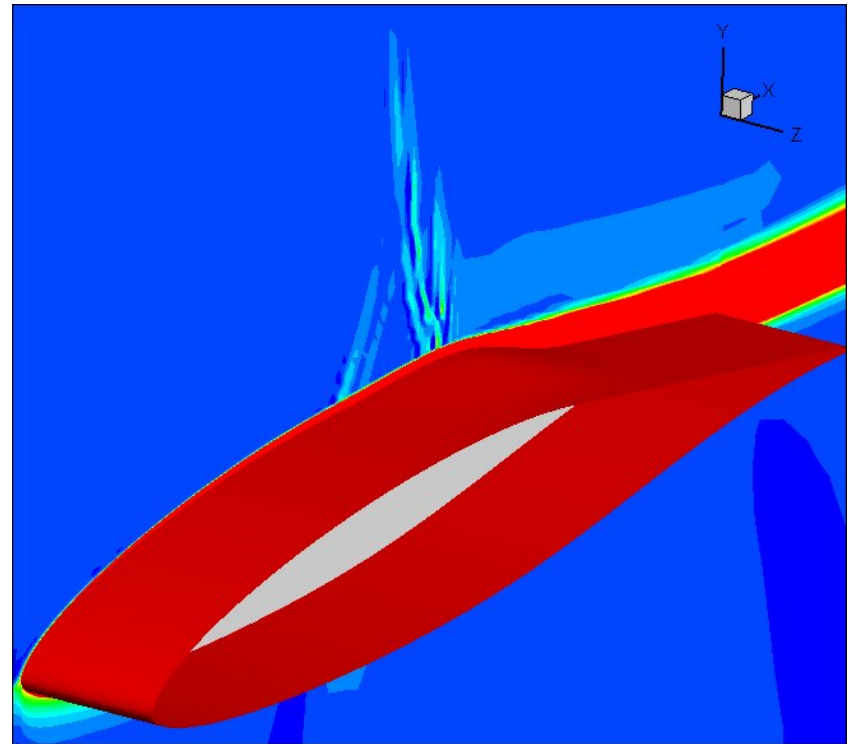
Objective function: C_D

<i>Bump Design</i>	Total Drag, C_D	Pressure Drag	Skin Friction Drag	Total Drag Reduction
Datum Aerofoil	0.01622	0.010630	0.005586	-
Optimised 2D Bump	0.01326	0.007563	0.005700	18.2%
Optimised 3D Bump	0.01296	0.007208	0.005756	20.1%

Entropy Contours

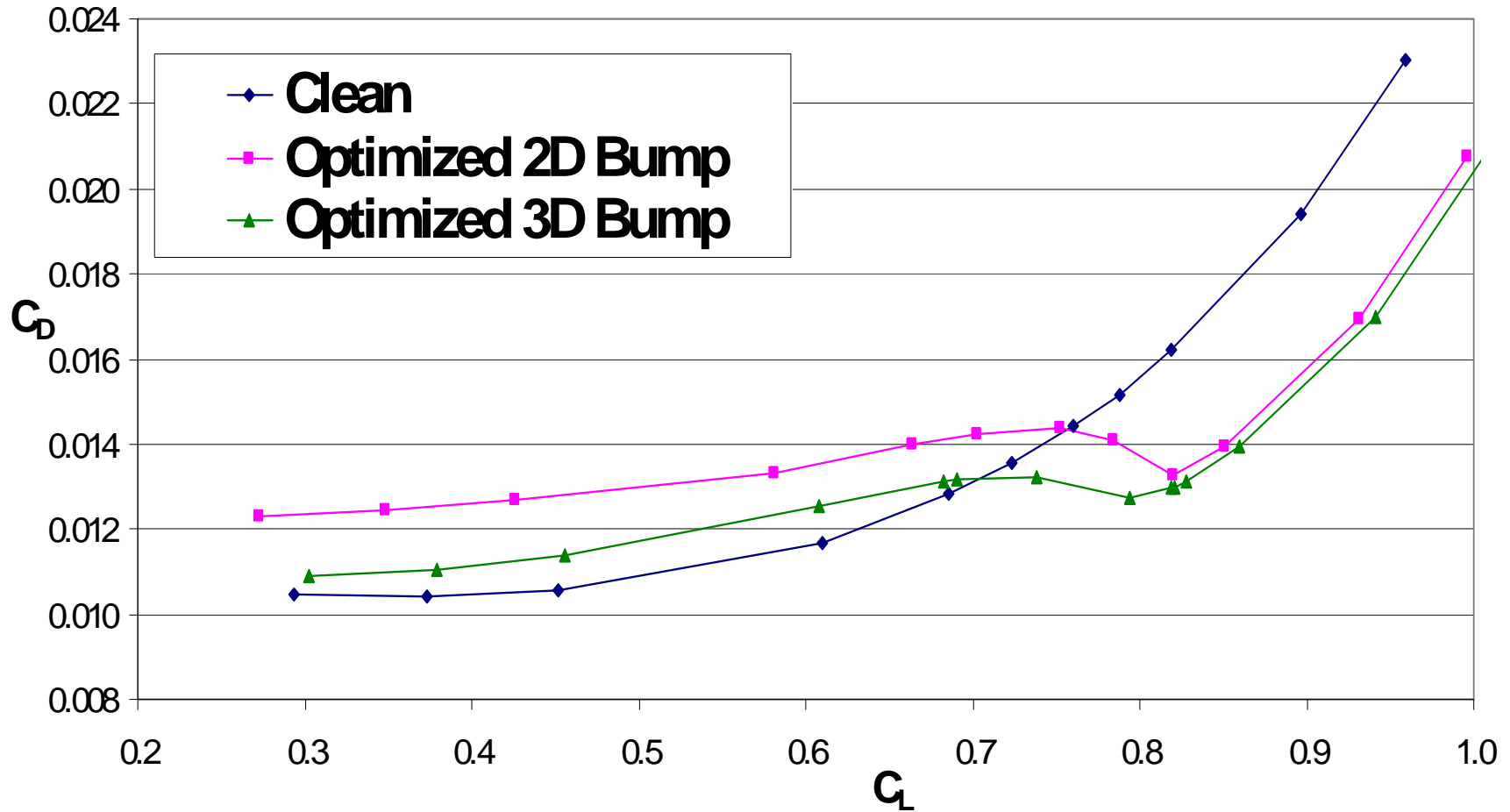


Datum Aerofoil

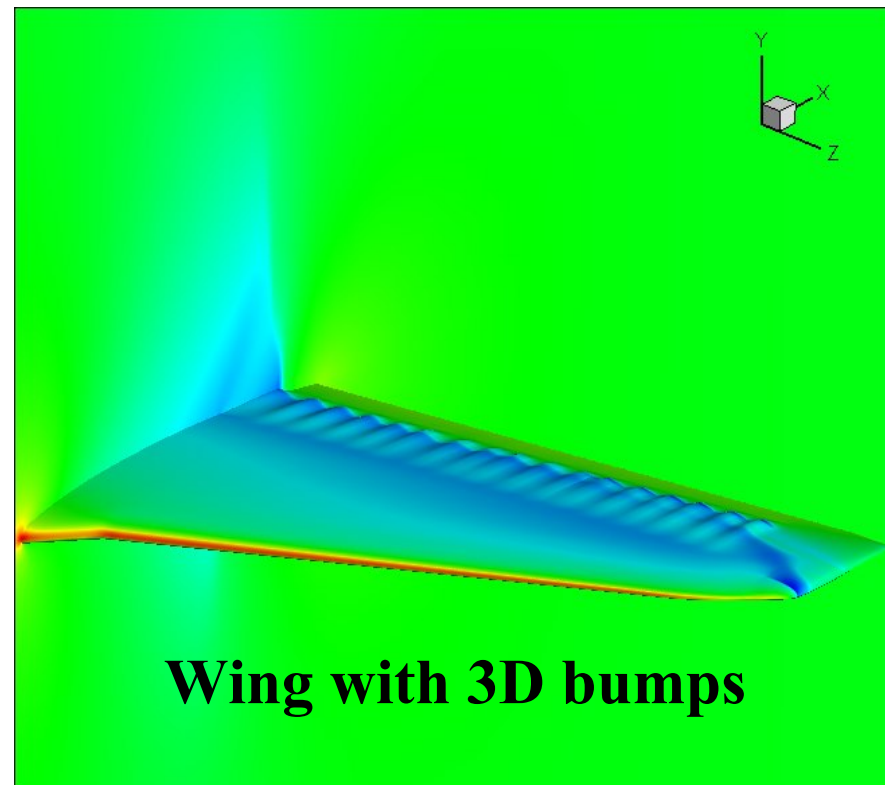
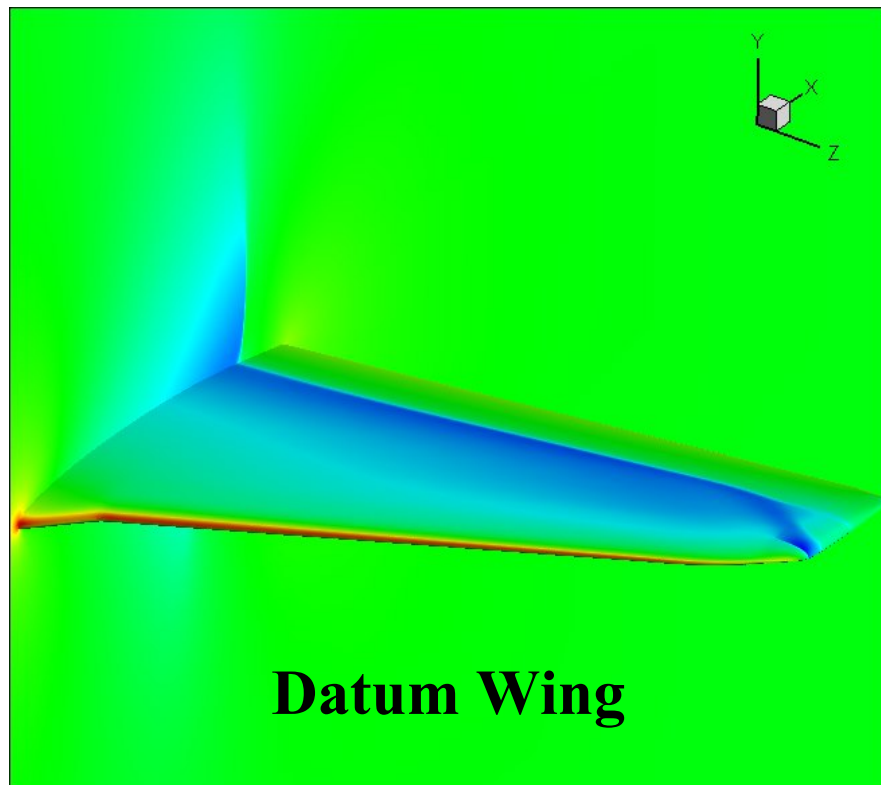


*Optimised 3D bump:
At the middle of the bump*

Performance over a range of C_L



3D Bumps on a 3D Swept Wing



$M = 0.85, Re_c = 20 \times 10^6, \alpha = 0.0$ Achieve 12% improvement in lift-drag ratio.

Optimisation on HPCx

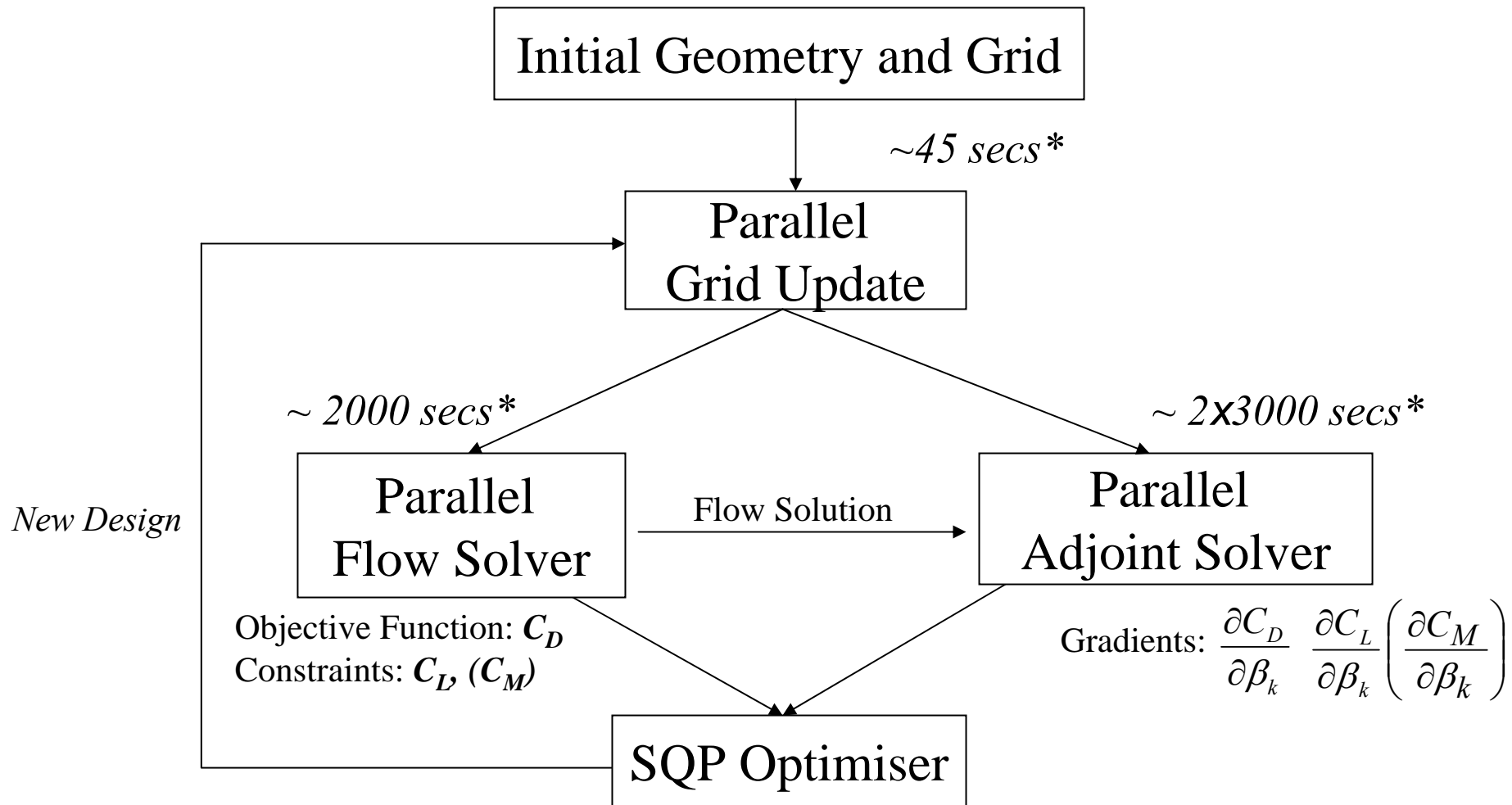
➤ Opportunities

- Much larger number of design variables
- Much finer meshes and more accurate flow/adjoint solutions
- Combine aerofoil profile optimisation at master sections with additional shock control bumps for transonic performance (can be viewed purposely tailored parameterisation)
- More detailed study of winglet optimisation in the context of the whole aircraft

➤ Code modifications

- From OpenMP to MPI: solver, adjoint, grid deformation
- Domain decomposition (not necessary for OpenMP)

Parallel adjoint-based optimisation



* Time estimated on 128 processors.

Flow solver: MERLIN

- ❑ Implicit structured multi-block or unstructured flow solver
- ❑ Advanced shock and shear layer capturing methodology for the solution of the Reynolds-averaged Navier Stokes equations.
- ❑ Various turbulence models: B-L, Curvature, S-A, $k-\omega$, SST, etc.
- ❑ The flow solver has been validated with various test cases



Parallelisation of MERLIN

- Exploit the multi-block structure of the code for the optimisation work
- The computational domain is divided into a number of size-balanced sub-domains, corresponding to the number of processors used on HPCx.
(METIS for the unstructured version)
- The exchange of information between the processors is performed using MPI non-blocking communications to avoid deadlock.

Discrete adjoint solver

- An efficient method for calculating sensitivity derivatives, especially for gradient based optimisation with large number of design variables
- Analytically differentiated for the calculations of the components of the Jacobians and the grid sensitivities.
- Derived for the multi-block version of MERLIN.
- Implemented with the Baldwin-Lomax algebraic turbulence model.
- The adjoint solver has been applied successfully for a range of optimisation problems including aerofoil shapes, the M6 wing, BWB shapes, 2D & 3D shock control bumps.

Parallelisation of the adjoint solver

- ❑ Implemented with the same parallelisation methodologies as in the flow solver when solving for the adjoint vectors, λ .
- ❑ The calculation of the sensitivity derivatives is looped over the number of design variables.(see later)
- ❑ Each calculation of the derivatives involves large and time-consuming matrix multiplications. Therefore parallelisation of this part is essential to avoid a bottleneck in the optimisation process when the grid resolution and the number of design variables are very large.
- ❑ In addition, the memory has to be distributed among the processors (data parallel) to avoid being limited by the memory of a single CPU or a single node, e.g. in the grid deformation module.

Parallelising the sensitivity derivative calculations

After the adjoint vectors are obtained, the sensitivity derivatives are calculated by:

$$\frac{dF}{d\beta_k} = \left(\frac{\partial F}{\partial \mathbf{X}} \right)^t \frac{d\mathbf{X}}{d\beta_k} + \boldsymbol{\lambda}^t \frac{\partial \mathbf{R}}{\partial \mathbf{X}} \frac{d\mathbf{X}}{d\beta_k} \quad (1)$$

Here, F is the objective function. The design variables are β_k , $k=1,2, \dots, K$. \mathbf{X} is the vector of the grid point coordinates. $\boldsymbol{\lambda}$ is the adjoint vector and \mathbf{R} denotes the residual vector in the flow solver.

From the above equation, it can be seen that the sensitivity derivatives needs to be calculated for all the design variables, which involves calculations of the grid sensitivities for all β .

Parallelising the sensitivity derivative calculations (cont)

Note that the grid sensitivity term $\frac{d\mathbf{X}}{d\beta_k}$ has to be calculated for each β_k .

- Each processor only stores the grid for its own block.
- However, β_k could have influences in multiple blocks.
- Therefore, each processors are provided with the complete surface grid modified by β_k .

The calculation of equation (1) can thus be performed separately but simultaneously by each processors. The values from each processors are summed up on the master processor to form the final value of the sensitivity derivative for β_k .

BWB Surface parameterisation and grid update

- Perturbation added to original geometry

$$y_{current} = y_{initial} + \delta y$$

- Perturbation parameterised by Bézier-Bernstein polynomials for the wing section shapes:

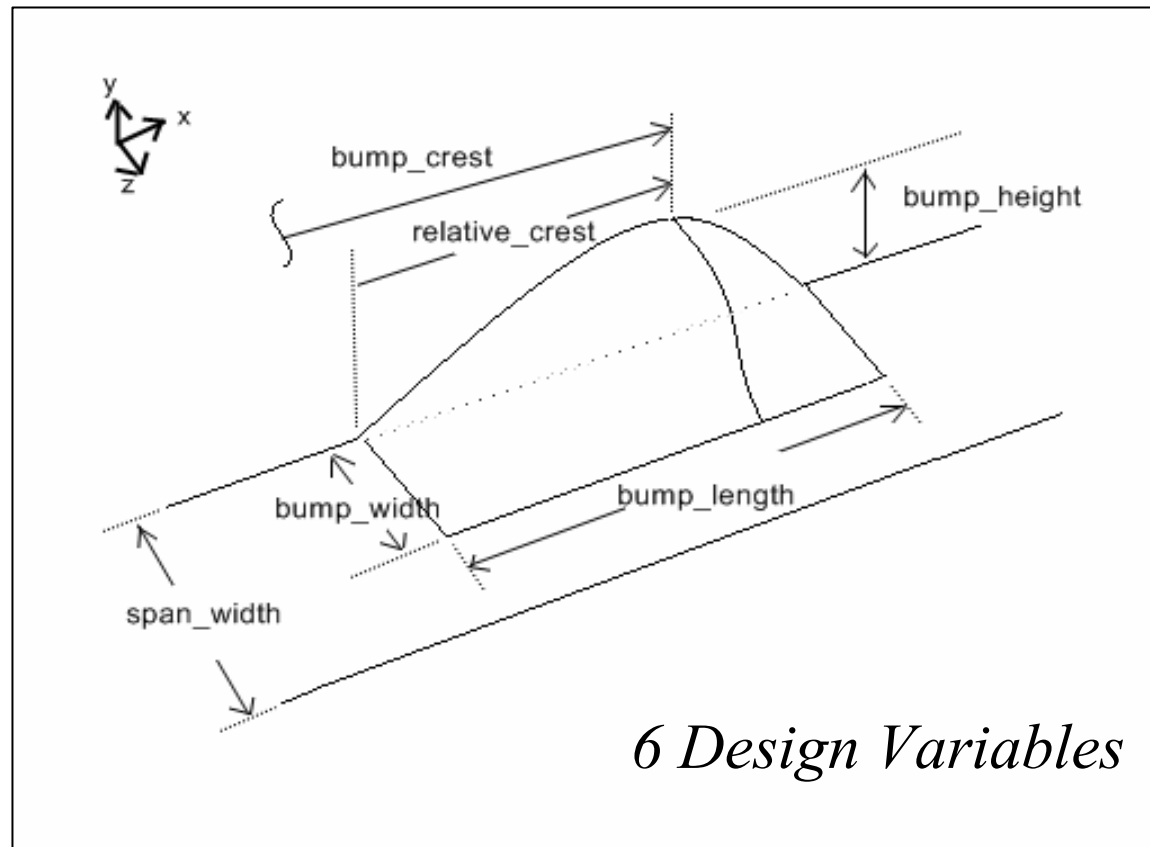
$$\delta y = \sum_{n=0}^N B_{n,N}(u) P_{y,n}$$

where $P_{y,n}$ are the $N+1$ design variables

- Analytical grid update: smooth transmission of the perturbation from the surface to the interior of the domain

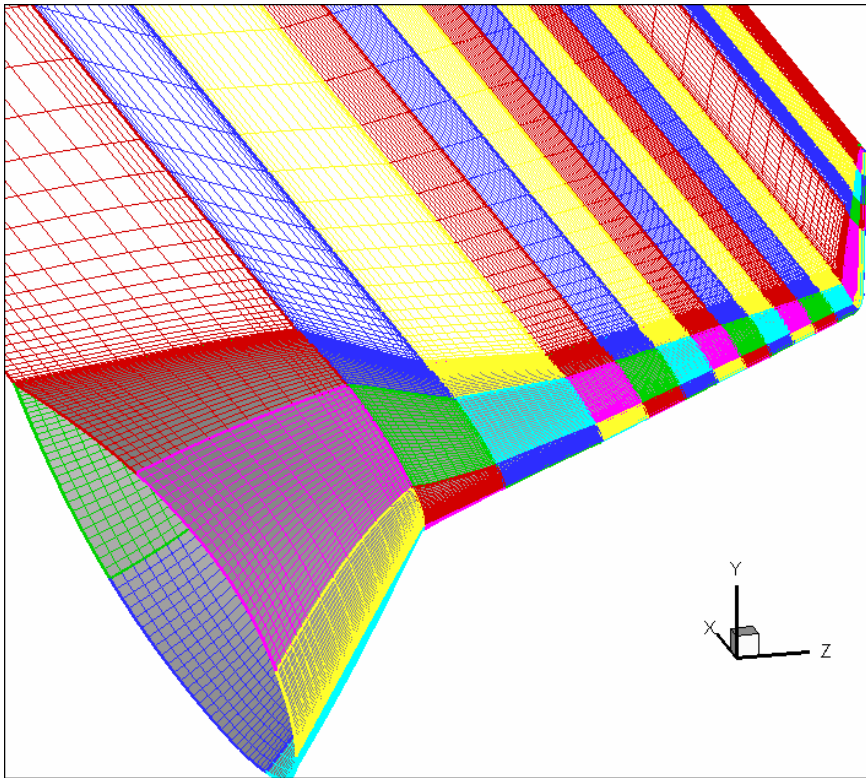
$$x_j^{new} = x_j^{old} + [1 - \text{arc}(j)] \times (x_{surface}^{new} - x_{surface}^{old})$$

Parameterisation of 3D bumps



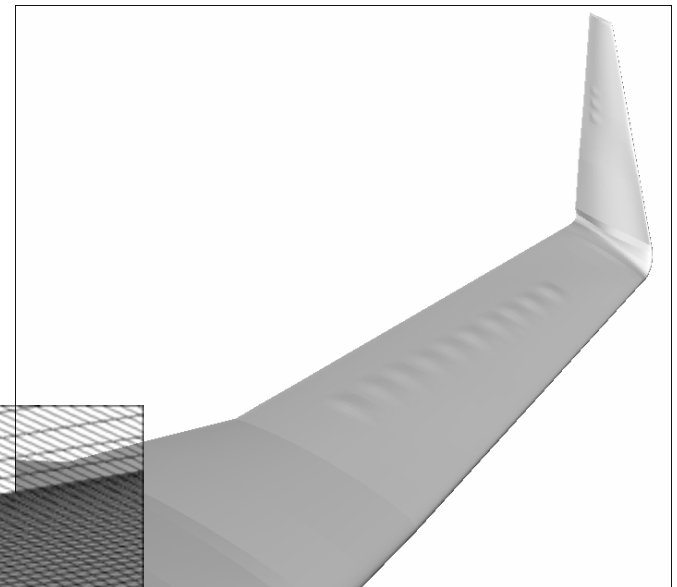
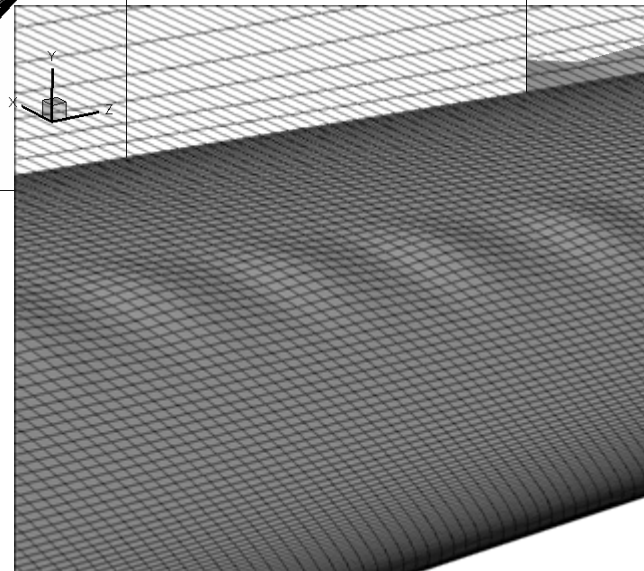
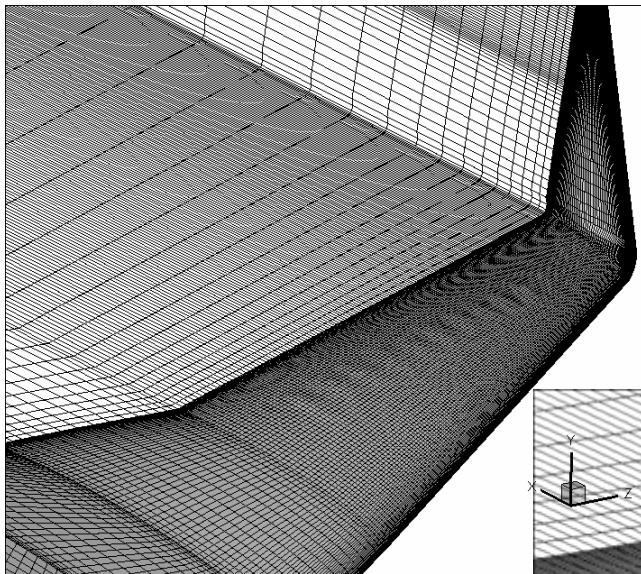
10 bumps on the outer wing &
3 bumps on the winglet

3D bumps on a BWB wing and grid requirement



- Only Euler calculations but the grid needs to be fine in the chordwise and spanwise direction to resolve the 3D bumps.
- $236 \times 33 \times 288 \approx 2.2$ million points. Whole optimisation can only be run on a large facility such as HPCx.
- Grid divided into 128 equal sized blocks to be run on the 128 processor queue on HPCx

3D bumps on a BWB wing and grid requirement



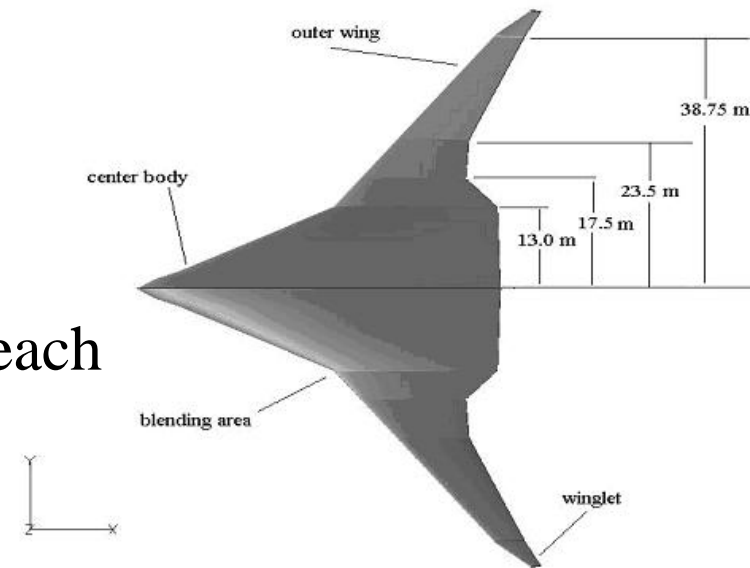
Euler optimisation of a BWB with 3D bumps

- **Optimisation problem:**

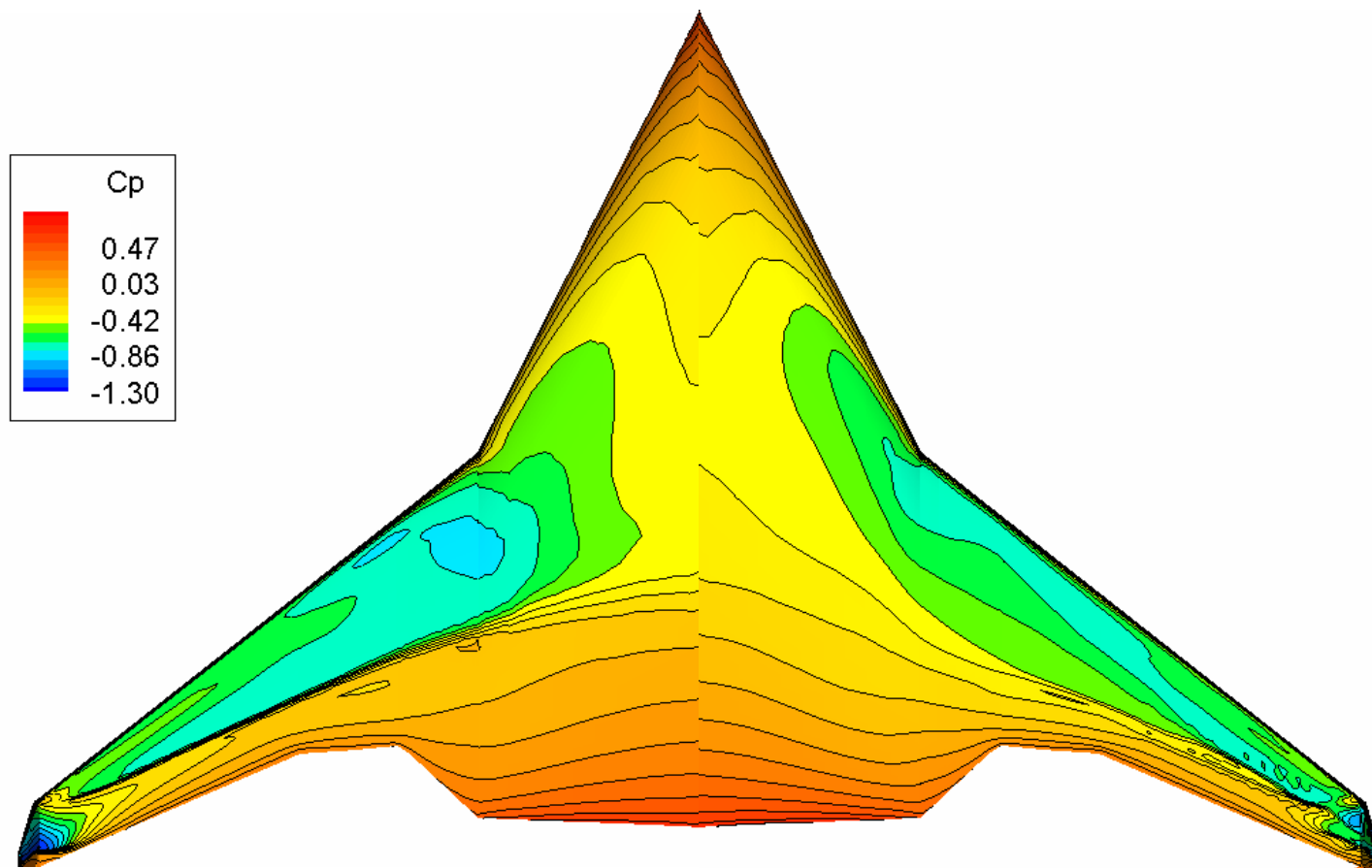
- Minimise C_D
- Lift constraint: $C_L > 0.41$
- 34 geometrical constraints on wing section area.

- **657 design variables:**

- 34 sections with 17 design variables each (16 Bezier parameters + twist).
- 13 3D bumps with 6 design variables each.



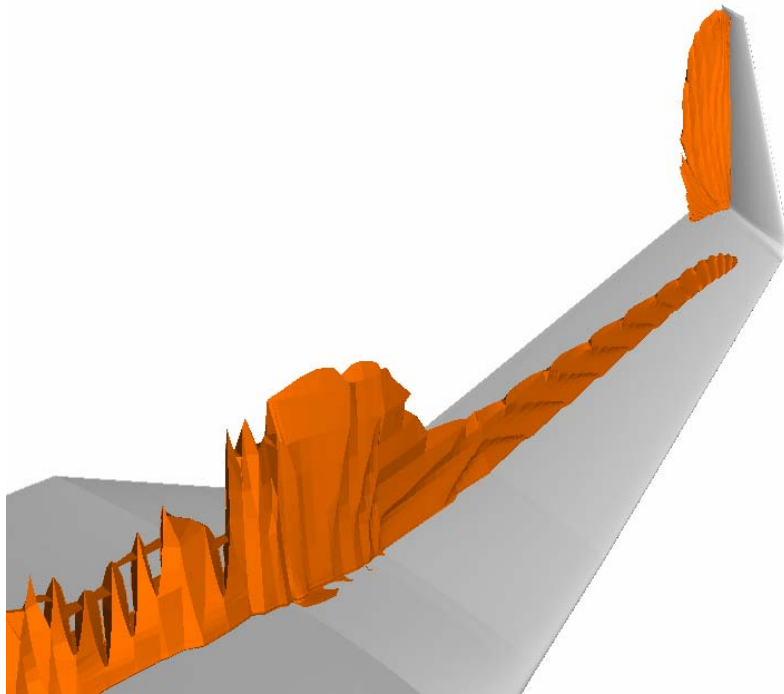
Optimisation cycles results



Original wing shape

4820th iteration cycle

Optimisation cycles results



Original wing shape

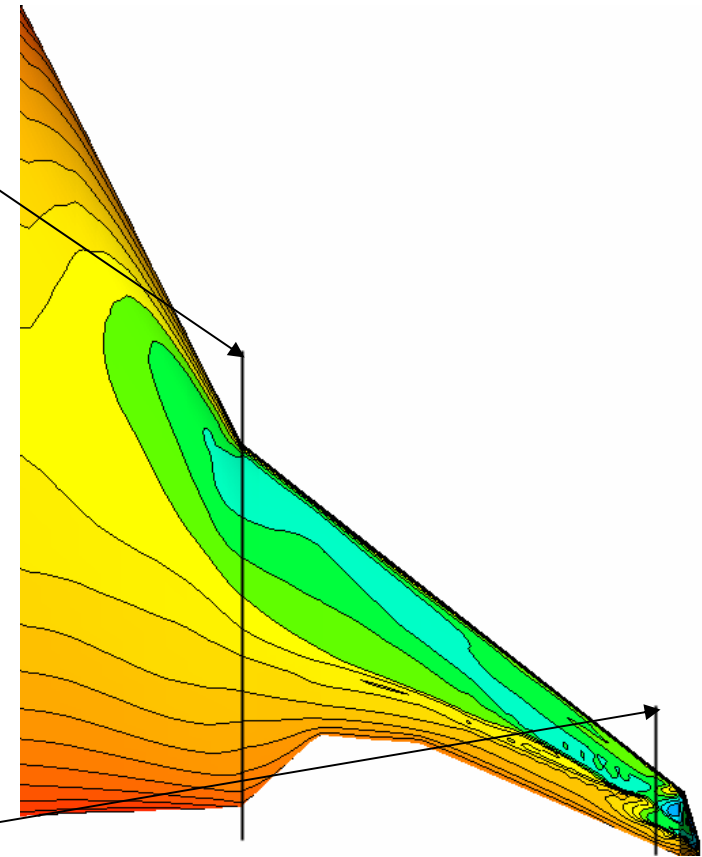
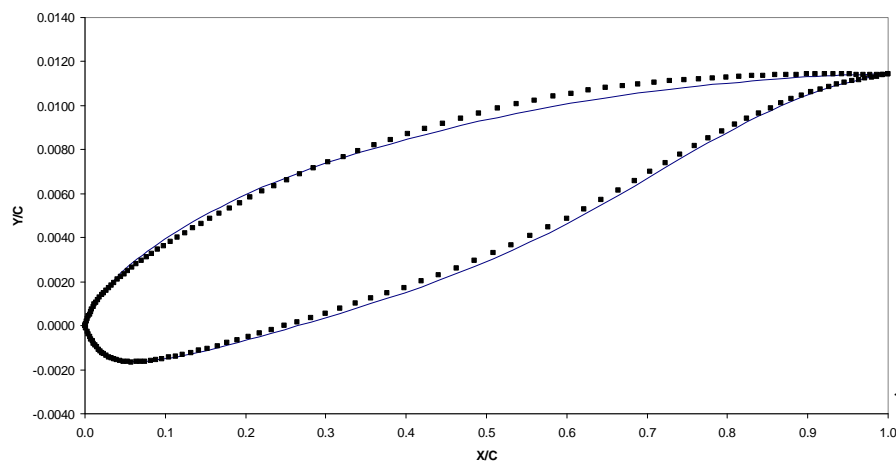
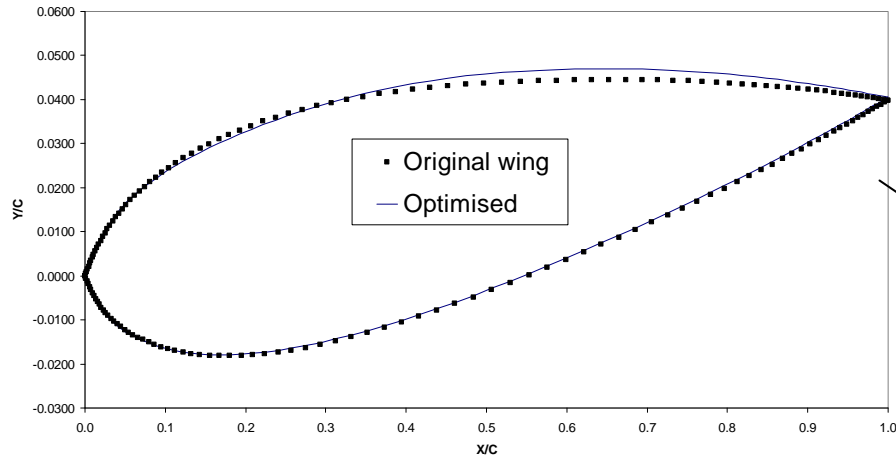


~~12~~th design cycle

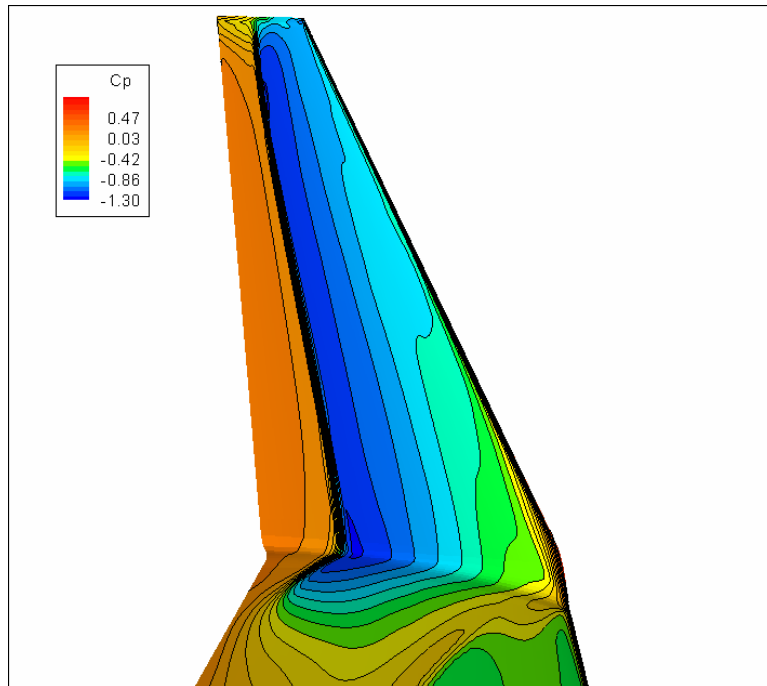
Comparisons of performances

	C_L	C_D	L/D	C_M
Initial	<i>0.4112</i>	<i>0.01554</i>	<i>26.46</i>	<i>0.09715</i>
1st design	0.4111	0.01414	29.08	0.1142
2nd design	0.4121	0.01359	30.33	0.1168
3rd design	0.4110	0.01330	30.91	0.1098
4th design	0.4104	0.01306	31.42	0.1133
5th design	0.4104	0.01295	31.70	0.1106
6th design	0.4104	0.01287	31.89	0.1107
7th design	0.4108	0.01284	31.98	0.1118
8th design	0.4119	0.01269	32.44	0.1145
9th design	0.4106	0.01244	33.01	0.1049
10th design	0.4103	0.01185	34.62	0.1090
11th design	0.4123	0.01170	35.24	0.1163
12th design	0.4123	0.01157	35.64	0.1170

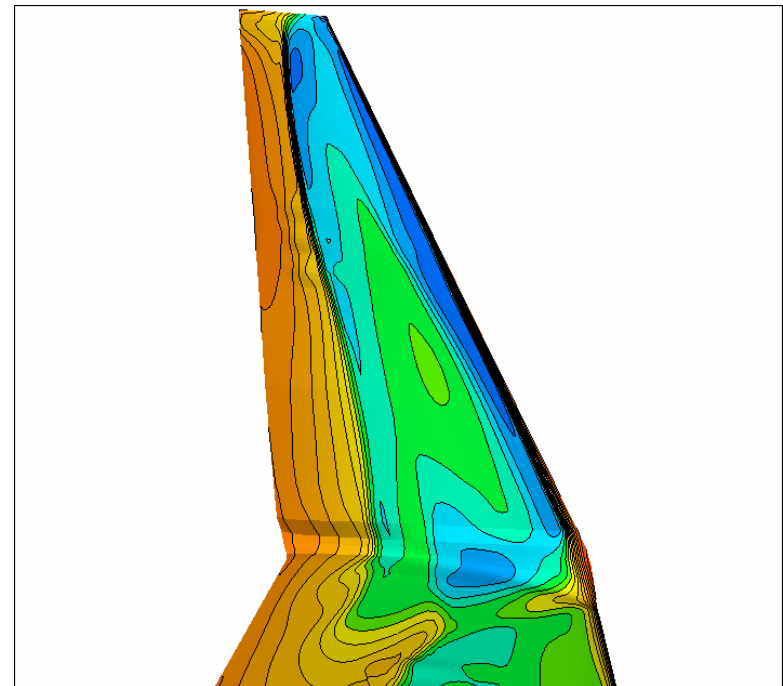
Optimised wing sections



Improvement at the winglet

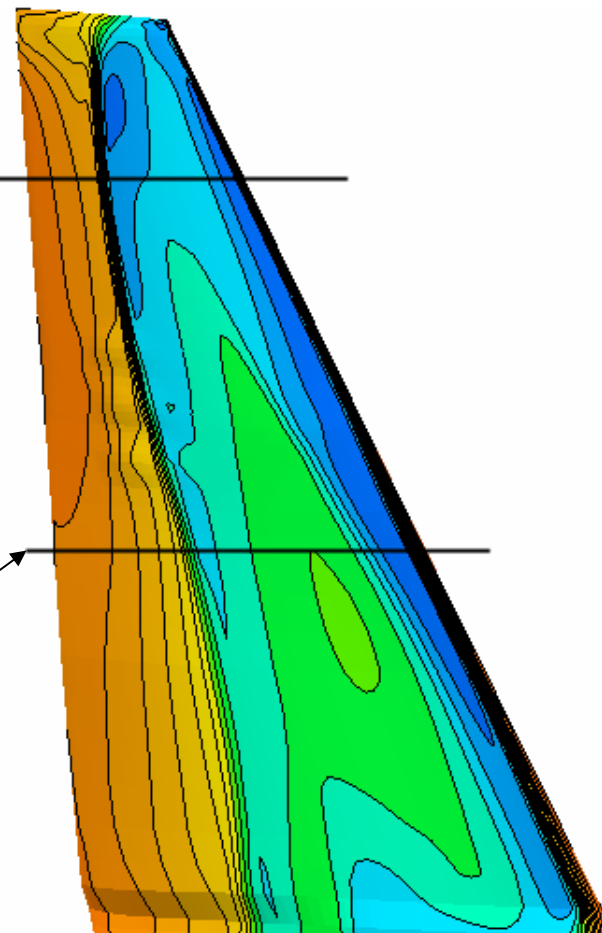
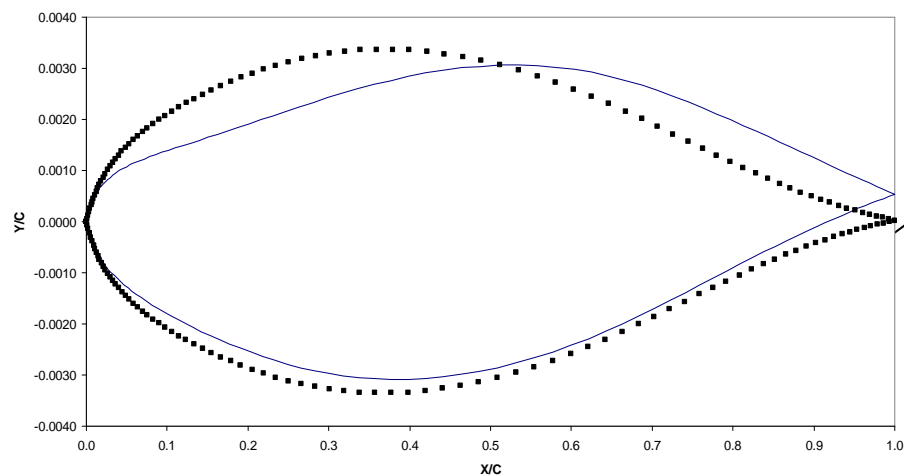
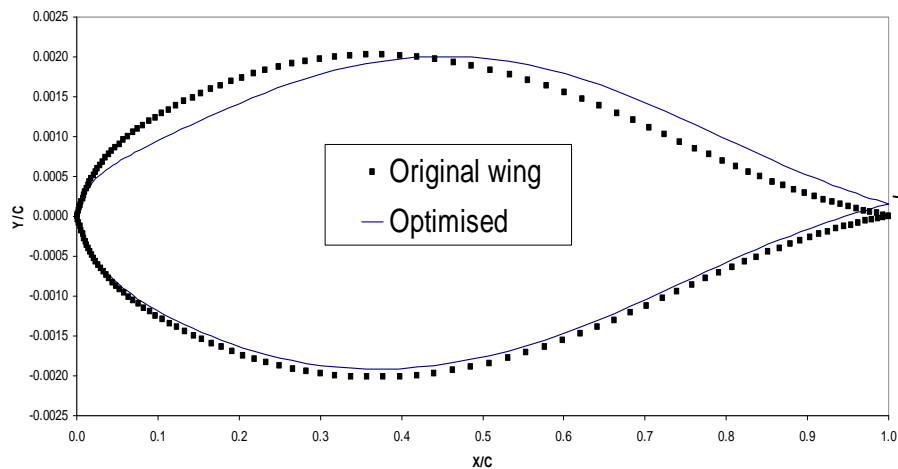


Original winglet



Optimised winglet (12th design)

Optimised winglet sections



Concluding remarks

- HPCx enabled a large aerodynamic optimisation be studied combining aerofoil profile optimisation with 3D shock control bumps with grid resolution over 2 million for over 650 design variables
- Although the optimisation cycles have not fully converged yet, it has shown some interesting improvement on the outer wing and the winglet with more than 25% drag reduction being achieved. Most visible is the weakening of the shock waves on the outer wing and the winglet.
- Substantial change of the winglet profile is produced by the optimisation with a slight twisting of the tip outwards. The strongest shock remains on the inside of the winglet and the bumps are yet to be further developed.
- A number of issues may be studied further: relative scaling of of the different design variables (e.g. bumps vs outer wing, wing vs winglet), robustness of the grid deformation, viscous optimisation for the shape, planform, and multi-disciplinary.



Acknowledgements

- EU for partially funding the adjoint and BWB work
- BAE Systems for funding the initial 3D shock control bump work (Technical monitor Dr Nick Sellars)
- Airbus for current funding of further development of shock control bumps (Technical monitors: David Saywers and Prof Norman Wood)
- EPSRC for HPCx usage within the UK-AAC.